ELSEVIER

Polymer 40 (1999) 5051–5062

polymer

Change of phase behaviour of SMA/PMMA blends during processing at high deformation rates

N.J.J. Aelmans[a,*], V.M.C. Reid[a], J.S. Higgins[b]

[a]*DSM Research, PCM-MP, PO Box 18, 6160 MD Geleen, The Netherlands*
[b]*Imperial College of Science, Technology and Medicine, Chemical Engineering Department, Prince Consort Road, London SW7 2BY, UK*

Received 1 June 1998; accepted 14 August 1998

Abstract

Processing of a SMA/PMMA blend through a capillary results in a complex change of phase behaviour with deformation rate. Both deformation induced demixing and remixing are observed. This complex phase behaviour as a function of apparent shear rate, is in qualitative agreement with experimental and theoretical results found for a polystyrene/poly vinyl methyl ether (PS/PVME) blend (Fernandez ML, Higgins JS, Horst R, Wolf BA. J. Polym. Sci. Polym. Lett. 1995;36(1)). In addition a different tongue shaped area of partially demixed material is observed in the current work (type *b*). This sample appearance is proposed to be related to the occurrence of vortices near the entrance of the capillary. This is a phenomenon which only occurs in contraction flow experiments. Pure shear rheological experiments, such as parallel plate or cone and plate, will not show such behaviour. The deformation induced demixing is spinodal phase separation. This is concluded from light microscopy experiments and via reheating experiments, showing that the blend needed only 15–25 s to remix. Preliminary results suggest that in addition to shear, elongation can cause dramatic changes in the blend phase behaviour. Capillary experiments are difficult to interpret because of the combination of shear, elongation, pressure and viscous heating. However, industrial scale blend processing such as injection moulding shows similar complexity. Hence capillary measurements are the best comparable small scale experiment. Future experiments will focus on modifying the capillary geometry, in order to discriminate between the influence of shear and elongation.

Keywords: Polymer blends; Shear flow; Elongational flow

1. Introduction

During the last two decades, extensive research has been published on the influence of shear on the phase behaviour of binary or ternary systems, both theoretically [2–9] and experimentally [1,10–24].

First shear induced mixing has been reported by several groups for several systems [2–4,10–16]. Subsequently shear-demixing has been observed [17–21]. More recent investigations have shown both shear-induced mixing and shear-demixing in the same system, leading to a very complex change of phase behaviour as a function of shear rate [1,5,6,22–24].

Theoretical considerations first lead to the addition of an extra term to the Flory–Huggins equation; the stored elastic energy E_s [5,6,18]. This phenomenological approach raises some fundamental questions concerning the physics. One of the most serious problems with this approach is that the thermodynamics of the system are described as if the system is in the stationary state. However, in reality the system is not in equilibrium, so non-equilibrium thermodynamics have to be used. Onuki [25], Hashimoto et al. [26], ten Brinke and Szleifer [27] and Doi and Onuki [28] have presented some fundamentally well thought out approaches, in which they study the migration of polymers in relation to concentration fluctuations [28], entropic and enthalpic aspects [27] and the kinetics of the shear induced change of phase behaviour [25]. A second point of interest is the fact that the approach of Wolf [18] is limited to pure shear. In industrial scale processing conditions combinations of shear and elongation occur. To handle these complex deformations in the approach the full deformation tensor has to be incorporated in the model. However, although Wolf's theory has some weak points, predictions of the change of phase behaviour of a polystyrene/poly vinyl methyl ether (PS/PVME) system with shear, showed a very complex phase diagram as a function of shear rate [5,6], in qualitative agreement with experimental work from Fernandez et al. [1]. Both shear induced mixing and shear-demixing are

* Corresponding author. Tel.: +31-46-476-7679; fax: +31-46-476-7569.

0032-3861/99/$ - see front matter
PII: S0032-3861(98)00702-2

Table 1
Characteristics of the polymers used in this work

Polymer	M_w (g mol^{-1})	M_w/M_n	T_g (°C)	Refractive index (n_D^{20})	wt% MA in SMA
STAPRON® SZ28110	110 000	1.93	162	1.574	28
STAPRON® SZ32080	82 000	1.71	171	1.570	32
DIAKON™ PMMA	104 000	1.92	116	1.492	—

observed for the same system. The approach seems to be useful, at least qualitatively. Hopefully new efforts will lead to the combination of the fundamentally well defined non-equilibrium thermodynamics approach [25–28] within the phenomenological approach [12].

Mainly experimental studies are limited to polymer solutions. These systems are chosen because they were well defined and not too complex, in addition they are easy to handle at room temperatures and can be studied using existing rheo-optical apparatus. In the polymer industry, most of the systems of interest are blends of two or more polymers in the melt at high temperatures of typically, 200°C–270°C. Because of the relevance to study systems in the melt, some work was done on the well known PS/PVME [1]. However, this system is still far from realistic for the polymer industry. Lyngaea-Jorgensen [15,16] studied an α-methyl-SAN/PMMA blend. This is the first industrially relevant system to be studied experimentally. To make this step to more realistic systems, equipment has to be upgraded to cope with the high temperatures, something very difficult for the rheo-optical techniques mostly used. The SMA/PMMA system (SMA: polystyrene-co-maleic anhydride), subject of the present investigation, does have its LCST within the relevant processing temperature window and has a large difference in the two components glass transition temperatures (T_g). The large difference in refractive index allows for visual (or optical) detection of the change of phase behaviour.

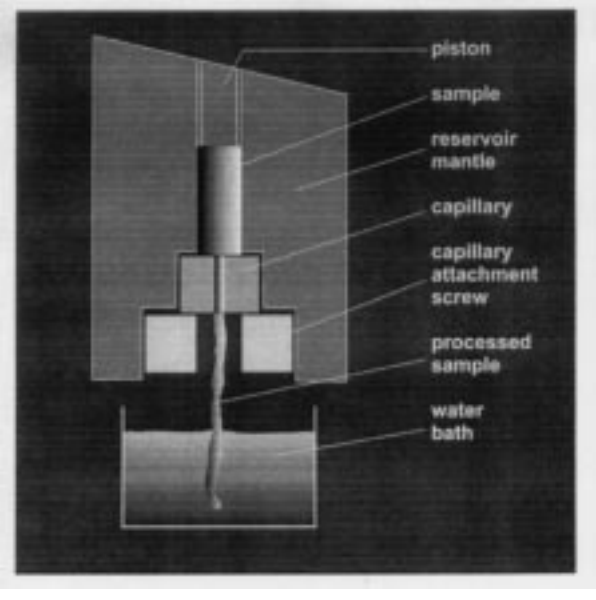

Fig. 1. Experimental set-up for quench experiments.

Also very important for experimental work on the influence of processing conditions on blend phase behaviour is to know which are realistic processing conditions used in industry. Most materials are extruded and injection moulded. Both shear and elongation do occur during extrusion and injection moulding processing processes. Additionally high pressures and viscous heating are involved, both factors known to be of influence on phase behaviour [29–31]. Most research up till now is concentrated on pure shear experiments as studied with cone and plate or parallel plate rheometers. However, Katsaros et al. [22] studied the influence of both pure shear and pure elongation on the phase behaviour of a PS/PVME blend. As industrial processing conditions involve both shear and elongation, capillary experiments were chosen for the experiments presented here, because the capillary is very comparable to the nozzle of the injection moulding machine. A motivation to investigate the influence of such deformations on blend phase behaviour is given by the occurrence of locally phase separated material observed in injection moulded SMA/PMMA blends.

2. Experimental

2.1. Materials

The polymers used in this work were STAPRON® SZ32080, a copolymer with styrene (S) and 32 wt% maleic anhydride (MA); produced on a commercial scale by DSM, and DIAKON™ PMMA, a PMMA with ethyl acrylate comonomer; supplied by ICI. Details on characteristics of both polymers are indicated in Table 1.

The blend investigated was a 20/80 (weight ratio) SMA/PMMA blend melt blended on a ZSK30 extruder. Prior to experimental study samples were dried under vacuum and nitrogen atmosphere at 80°C until dry.

2.2. Instrumentation

2.2.1. Rheometers

The flow curves of both pure materials and their 20/80 blend were measured on a Göttfert Viscotester 1500 and a Göttfert Rheograph 2002. The Göttfert Rheograph 2002 was used to extrude the SMA/PMMA blend with a given piston speed through a 30/1 capillary with a 180° entrance angle. The sample coming out of the capillary was quenched

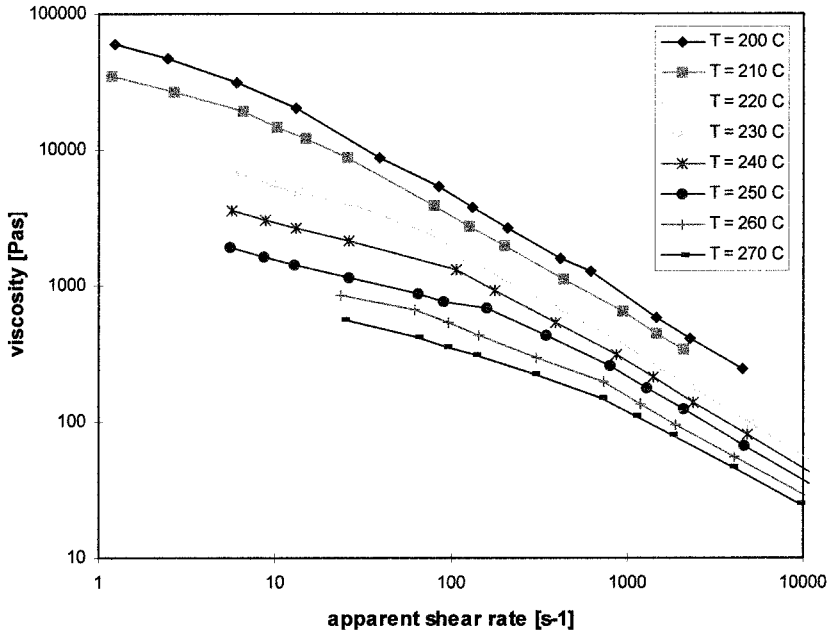

Fig. 2. Flow curves of DIAKON™ PMMA.

immediately in a water bath, as illustrated in Fig. 1. All materials used were granules and were heated for 6 min in the rheometer reservoir before starting the experiment.

Apparent shear rates ranging from about 0.6 s^{-1} to about 25 000 s^{-1} were applied by varying the piston speed. After each high piston speed, the piston speed was significantly lowered in order to relaxate any high shear history, after which the piston speed was further increased to obtain a sample processed at higher piston speed. Temperatures used ranged from 190°C to 230°C. Each experiment was performed at constant temperature and for a limited range of apparent shear rates. After each experiment the reservoir had to be cleaned and refilled. Reproducibility was investigated via experimental runs with overlapping shear rates.

2.2.2. Injection moulding

A 20/80 SMA/PMMA blend with a STAPRON® SZ28110 was injection moulded on a Arburg CMD067

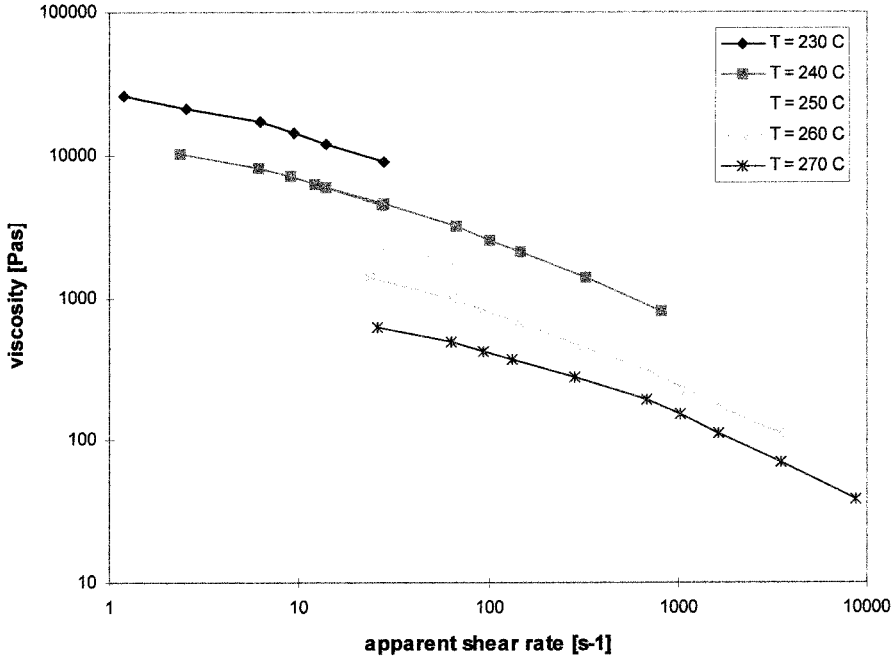

Fig. 3. Flow curves of STAPRON® SZ32080.

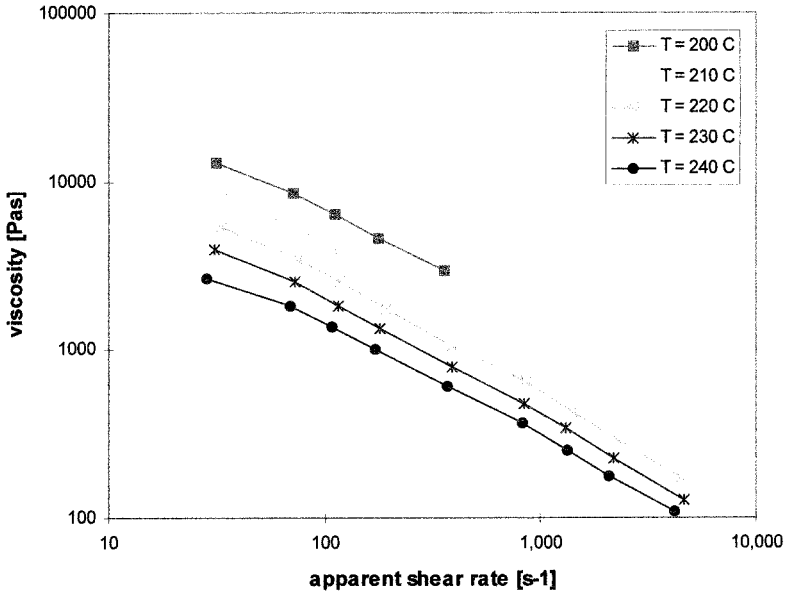

Fig. 4. STAPRON®/DIAKON™ 20/80 blend flow curves.

injection moulding machine at a melt temperature of 250°C and variable injection times.

2.2.3. Phase contrast light microscopy

The quenched samples were further examined by phase contrast light microscopy. Some cross sections of the extruded samples were investigated on a Zeiss Axiophot microscope with a 640 × magnification and photographed.

2.2.4. Differential scanning calorimetry (DSC)

Quenched samples were investigated by DSC. A heating rate of 20°C/min was used. The first heating curve ended at a temperature of 180°C, the second heating curve ended at 250°C. Second heating curves are reported.

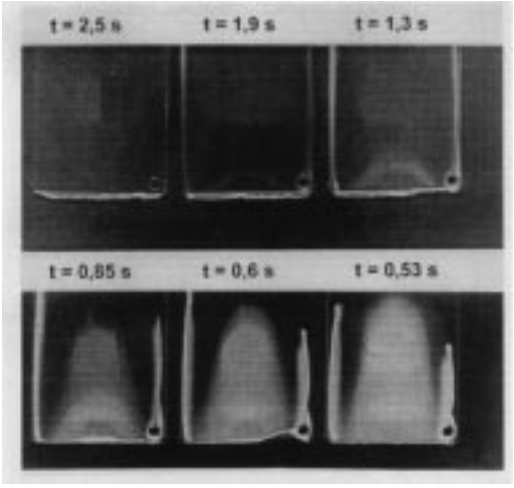

Fig. 5. Injection moulded STAPRON® SZ28110/DIAKON™ 20/80 blend at $T = 250$°C, different injection times.

3. Results

3.1. Rheology

Flow curves of the DIAKON™ PMMA, STAPRON® SZ32080 and the 20/80 SMA/PMMA blend are shown in Figs. 2–4 respectively. STAPRON® SZ28110 was only used for injection moulding tests and not characterised further.

The STAPRON® SZ32080 is a much more viscous material than the DIAKON™ PMMA as one can see from the flow curves. STAPRON® SZ32080 could not be measured at temperatures below 230°C, because the force on the piston became too high and the pressure transducers reached their upper limit (2000 bar). For the same reason, viscosities could not be measured at higher shear rates. From Fig. 4, one can see that the blend viscosity is between that of PMMA and SMA.

3.2. Injection moulding experiments

A 20/80 SMA/PMMA blend with a STAPRON® SZ28110 was injection moulded on an Arburg CMD 067 injection moulding machine. Melt temperature was kept constant at about 250°C and injection times were changed from 0.5 s up to 4.0 s. In order to keep melt temperature constant for all different injection times, the cylinder temperatures had to be adjusted accordingly from experiment to experiment. Fig. 5 shows the sample appearance after injection moulding the same blend composition at different injection times and similar melt temperatures.

Opaque lines can be observed in the transparent sample positioned at the sides of the sample. From these results it can be concluded that blend phase behaviour is very

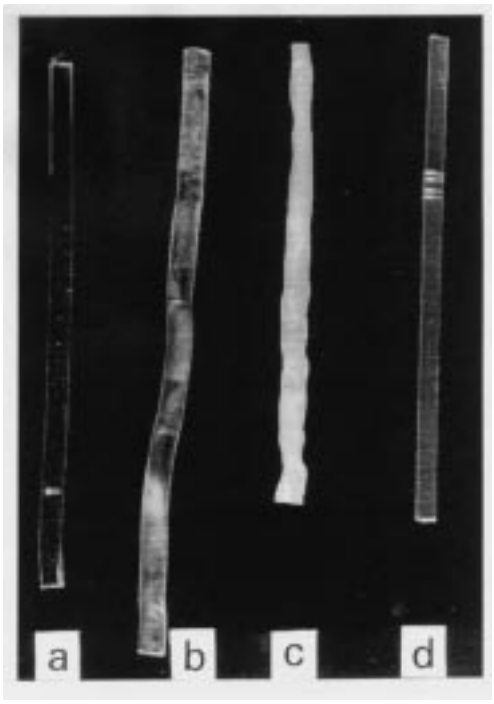

Fig. 6. Four typical sample appearances from quench experiments on the rheometer, STAPRON® SZ32080/DIAKON™ 20/80 blend.

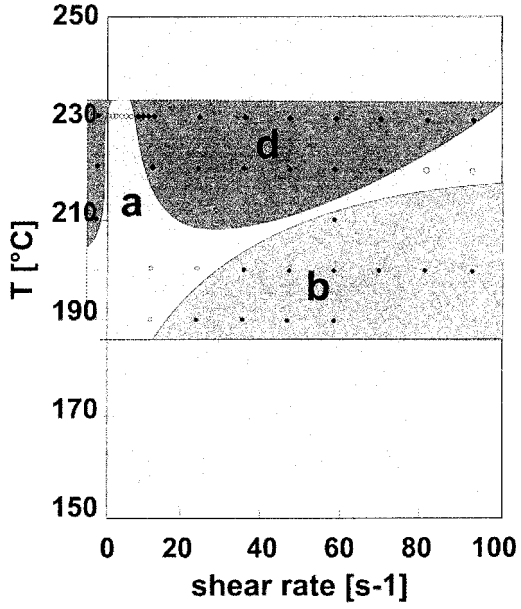

Fig. 7. Visual phase diagram of STAPRON® SZ32080/DIAKON™ as a function of apparent shear rate in a 30/1 capillary, 180° entrance angle, shear rate = 0–100 s^{-1}. Shaded areas labelled a, b or d correspond to a sample appearance as indicated in Fig. 6. Dark symbols are (partially) demixed processed samples, transparent symbols are transparent miscible samples.

sensitive to high (around 25 000 s^{-1}) deformation rates. Both shear and elongation have their influence on blend phase behaviour. The occurrence of the opaque lines was thought to be related to shear rates in the mould, as described previously [32]. Subsequent to further study, the opaque lines are currently proposed to be related to nozzle geometry used and stagnation points in the mould, in combination with the relaxation times needed for the demixed material to remix again. These phenomena will be fully discussed in a second paper [33]. The aforementioned injection moulding observations are the motivation to perform the capillary experiments as discussed in the following sections. The capillary experiments show clearly what happens in the injection moulding nozzle.

3.3. Quench experiment on the rheometers

Quench experiments were performed at temperatures between 190°C and 230°C with steps of 10°C in between. At a certain temperature, the measurement started with the lowest piston speed available and the piston speed was slowly increased. After each piston speed applied, the piston speed was lowered to the lowest available and kept at that speed until all pressures had relaxed and the sample appearance was the same as observed for that (very slow) piston speed before. Then the piston speed was raised again to another piston speed. This continued until the reservoir was empty. Residence time of the sample in the reservoir was considered, with the result that for the low shear experiments only part of the reservoir volume was used for the experiment and the rest was discarded. Samples were quenched immediately in a water bath and coded for further investigations.

The quench experiments resulted in four typical sample appearances as illustrated in Fig. 6. Sample *a* is a transparent miscible sample, while sample *d* is a hazy phase separated sample. For samples classified *c* the phase separation even leads to opacity of the material. A very strange sample appearance was observed for samples classified as *b*. These samples are in principle transparent miscible samples, but a small amount of bluish/opaque material is observed as a spiral around the cylindrical axis of the sample. This sample appearance has raised a lot of questions and is discussed thoroughly in the discussion section.

The visual observations are a very good indication for the phase behaviour of a given sample, because the refractive indices of SMA and PMMA are very different. Even the slightest phase separation results in a hazy appearance.

If the quenched samples are investigated visually, a phase diagram as a function of apparent shear rate can be constructed. Figs. 7–9 show these visual phase diagrams for apparent shear rates of 0–100 s^{-1}, 0–1000 s^{-1} and 0–25 000 s^{-1} respectively. A filled symbol indicates a phase separated sample of type *b*, *c* or *d*, an open symbol indicates a transparent miscible sample.

In these figures the lines and shaded areas are drawn to

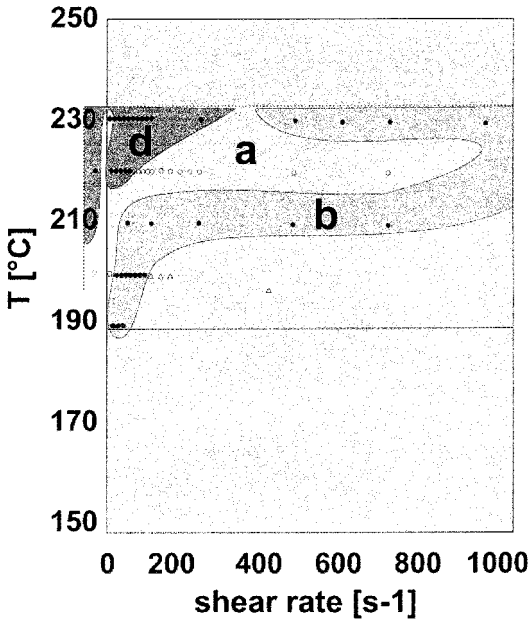

Fig. 8. Visual phase diagram of STAPRON® SZ32080/DIAKON™ as a function of apparent shear rate in a 30/1 capilalry, 180° entrance angle, shear rate = 0–1000 s^{-1}. Shaded areas labelled a, b or d correspond to a sample appearance as indicated in Fig. 6. Dark symbols are (partially) demixed processed samples, transparent symbols are transparent miscible samples.

guide the eye. The shaded areas are marked with *a*, *b*, *c* or *d*, in order to illustrate the sample appearance. Left of the temperature axis the stationary phase diagram (without applying any deformation) is given. This was determined by heating some blend granules in the DSC to a certain temperature at 10°C/min and then quenching the sample below its T_g. The DSC pan was opened and the sample appearance was assessed visually. Similar results were obtained by light scattering experiments.

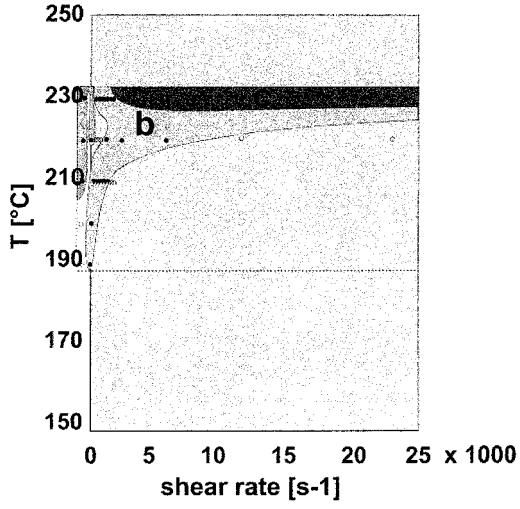

Fig. 9. Visual phase diagram of STAPRON® SZ32080/DIAKON™ as a function of apparent shear rate in a 30/1 capillary, 180° entrance angle, shear rate = 0–25 000 s^{-1}. Shaded areas labelled b or c correspond to a sample appearance as indicated in Fig. 6. Dark symbols are (partially) demixed processed samples, transparent symbols are transparent miscible samples.

At temperatures of 220°C or 230°C one can observe a complex change of phase behaviour with shear rate. In the stationary state the blend is a two phase system, while very moderate apparent shear rates transform the blend to a transparent miscible system. Further increase of the apparent shear rate (10–15 s^{-1}) induces the system to phase separate again and at apparent shear rates around 70–100 s^{-1} the blend becomes miscible again. This means that both deformation induced mixing and demixing occur in the same blend system. Fig. 10 shows how phase behaviour can change instantly when changing the piston speed applied. Here the low piston speed of 0.01 mm/s is followed by a piston speed of 5.0 mm/s (left) or 10.0 mm/s (right), without removing the sample processed at 0.01 mm/s, showing an immediate change in phase behaviour in one processed and quenched sample from slightly demixed to completely opaque. Recent experimental investigations by Katsaros et al. [22], Hindawi et al. [23] and Fernandez et al. [24], showed similar complex phase diagrams for a PS/PVME system. Theoretical work of Horst and Wolf [5,6], combined with experimental work of Higgins et al. [1] showed similar results. The only qualitative difference in the shape of our phase diagram, and that found for the PS/PVME system, is the strange tongue shaped area marked with *b*. As these samples show a very varied appearance, this makes the phase diagram very complex. This will be discussed thoroughly in the next section.

Most probably the deformation induced phase separation has a co-continuous spinodal structure. This can be concluded from light microscopy (see next section) and from a reheating experiment. During the reheating experiment, a quenched deformation induced phase separated blend is heated again above its T_g but below the cloud point temperature. It took about 15–25 s for the material to remix again. A binodal phase separated sample with a disperse morphology would require more time to remix, in addition to mechanical remixing.

3.4. Differential scanning calorimetry (DSC) measurements

DSC measurements were performed on several samples. Fig. 11 shows the DSC curves of a transparent sample, type *a*, processed at $T = 230$°C and 0.576 s^{-1} and a bluish hazy sample, type *d*, processed at $T = 230$°C and 11.57 s^{-1}. The type *a* sample clearly shows a single T_g, while the type *d* sample shows two different T_gs. These DSC measurements confirm the visual interpretation of these samples. Other type *d* samples did not show these two T_gs so clearly as for this sample. Probably there was too much material of a PMMA-rich phase compared to the SMA-rich phase to observe a second T_g. Fig. 12 shows the DSC curves of a type *b* sample and a type *c* sample. No clear second T_g can

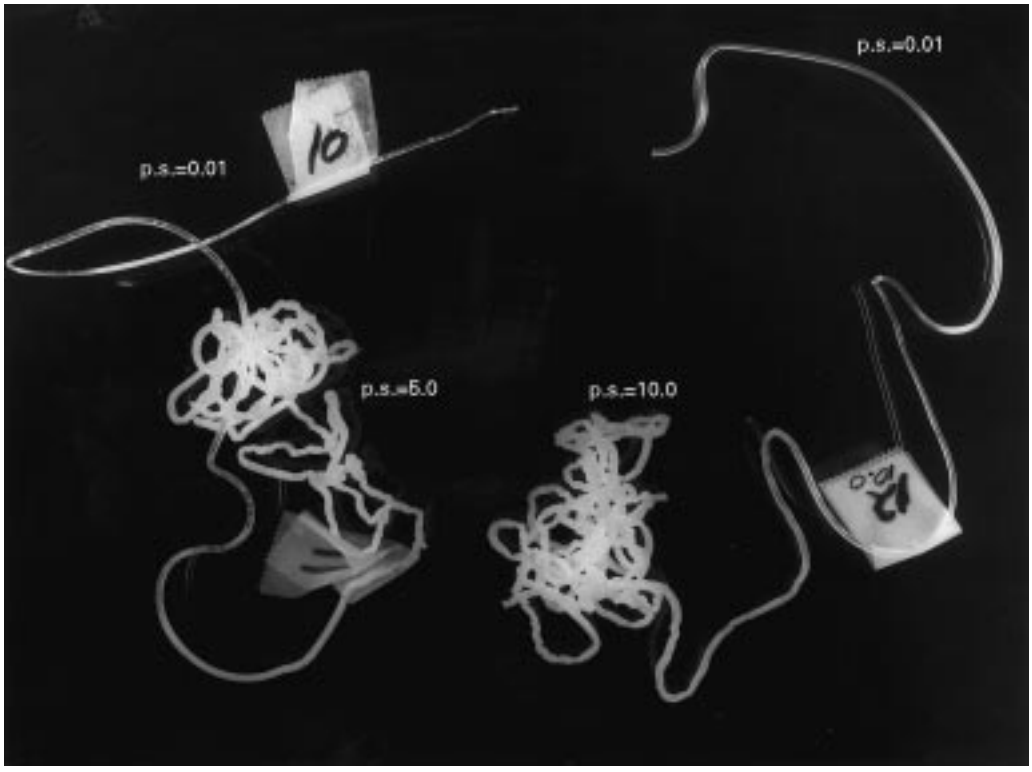

Fig. 10. Change of phase behaviour with instantly changing the piston speed applied. p.s. = 5.0 mm/s (left) and p.s. = 10.0 mm/s, (right).

be observed in the type *b* curve, indicating that the amount of bluish material wrapped around the transparent material present is a minor component compared to the transparent bulk, that it cannot be discriminated within a DSC measurement. The type *c* sample shows a strange DSC curve, which can only be explained as two (or more) overlapping T_gs. These DSC measurements illustrate that the DSC technique is not sufficiently sensitive to probe the blend phase behaviour as is the visual observation of the sample appearance. For this reason the phase diagram as a function of apparent shear rate (Figs. 7–9) is based on visual observations of the sample appearance.

A type *c* sample, quenched after processing, was reheated in a DSC cup for variable time periods and quenched again in the DSC, each time using a fresh type *c* sample processed under the same conditions. Measurements were performed

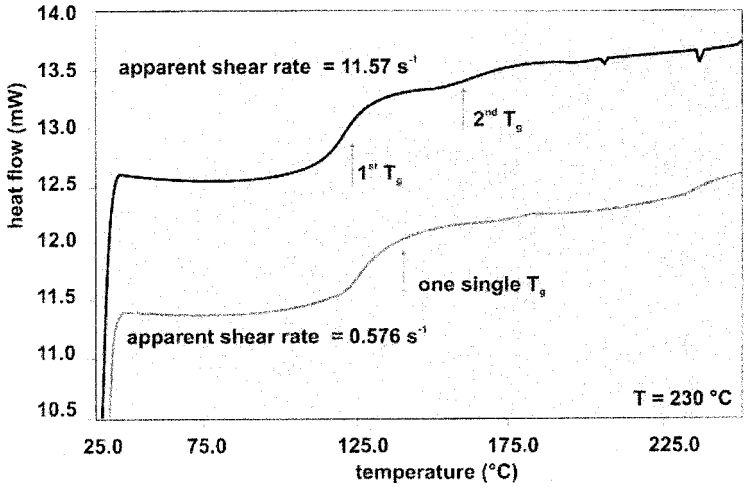

Fig. 11. DSC curves of a transparent sample, type *a*, processed at $T = 230$°C and 0.576 s^{-1} and a bluish hazy sample, type *d*, processed at $T = 230$°C and 11.57 s^{-1}.

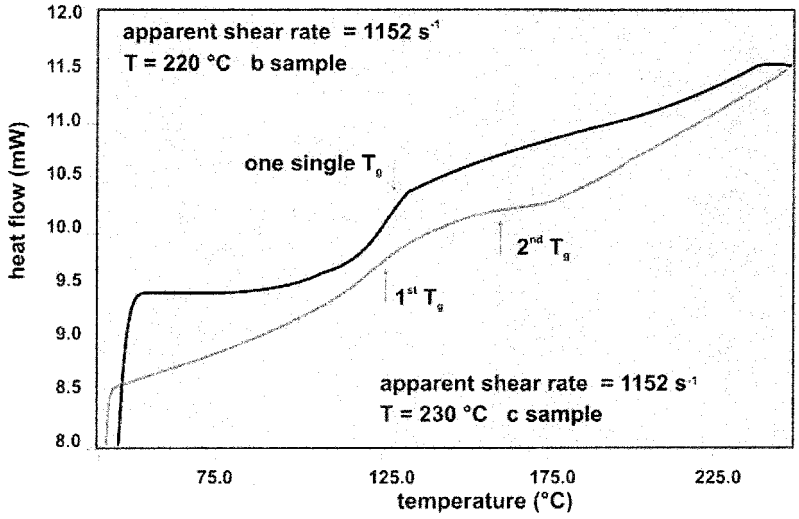

Fig. 12. DSC curves of a type *b* sample and a type *c* sample.

at 15, 30, 60, 300 and 600 s. It was found that the type *c* samples partially remixed within 30 s at $T = 190°C$ and completely remixed at 60 s at $T = 190°C$. As this remixing occurs very rapidly at low temperature, this might indicate that the type *c* samples are spinodally demixed. Obviously deformation induced phase separation has a spinodal character.

DSC measurements on the injection moulded samples of the 20/80 STAPRON® SZ28110/DIAKON™ PMMA blend are shown in Fig. 13.

The opaque material is demixed (2 T_gs), but the T_gs are very close to each other. The transparant blend material gives a single T_g.

3.5. Light microscopy

Three different samples processed as described earlier were investigated by light microscopy. All three samples were processed at $T = 230°C$, but at different piston speeds (p.s.); p.s. = 0.001 mm/s, p.s. = 0.1 mm/s and p.s. = 10.0 mm/s respectively. The phase behaviour observed is shown in Fig. 14. One can clearly observe a homogeneously mixed blend at p.s. = 0.001 mm/s and spinodally demixed phase behaviour at p.s. = 0.1 mm/s and 10.0 mm/s respectively. The latter has a more pronounced oriented morphology because of the high processing speeds applied. These microscopy results are in agreement with the visual

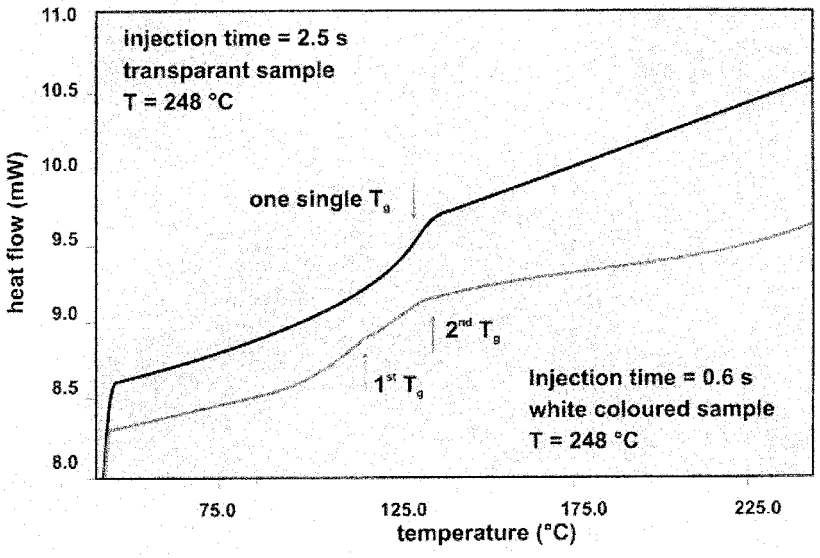

Fig. 13. DSC curves of injection moulded 20/80 STAPRON® SZ28110/DIAKON™ blend.

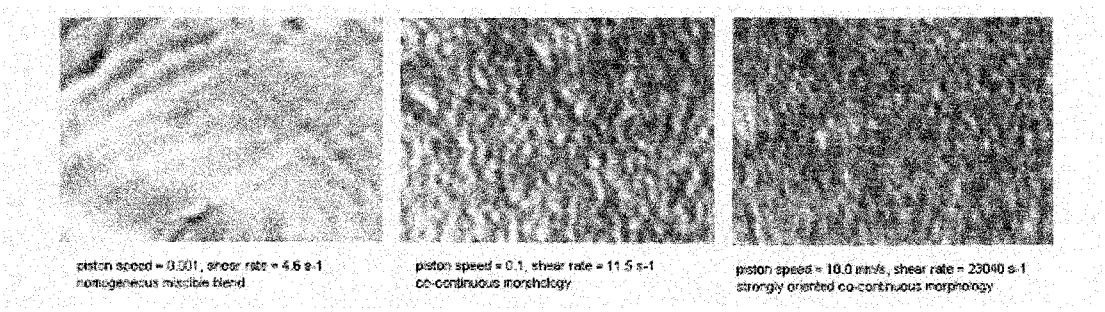

Fig. 14. Light microscopy on 3 different samples.

interpretation of the blends phase behaviour as indicated in Figs. 7–9.

4. Discussion

As described in the previous section, the change of SMA/PMMA phase behaviour with apparent shear rate was found to be very complex (please note that an apparent shear rate is used as calculated from the piston speed applied. In reality both shear and elongation are applied to the sample). The shape of the temperature/shear rate phase diagram is in qualitative agreement with experimental results from Fernandez et al. [1,24] and with a predicted shape as described by Horst and Wolf [1,5,6]. Horst and Wolf predicted shear mixing and redemixing as a function of shear rate at constant temperature in a way as observed in our experiments. However, there are three large discrepancies between our experimental diagram and the earlier mentioned references. The first, concerns the shape of the diagram. For SMA/PMMA an additional tongue shaped area was found with samples of type *b* (see Figs. 7–9), which was not observed nor predicted for the PS/PVME. Some modelling from Horst [34] (unpublished results) on this SMA/PMMA system also did not show this additional tongue shaped area, but did show qualitative agreement with the rest of the experimental diagram (Figs. 7–9).

It is believed that the samples with the bluish curl (type *b*) show a phenomenon related to contraction flow. When a material is processed through a contraction, the material is elongated at the contraction and vortices are formed at the edges as illustrated in Fig. 15.

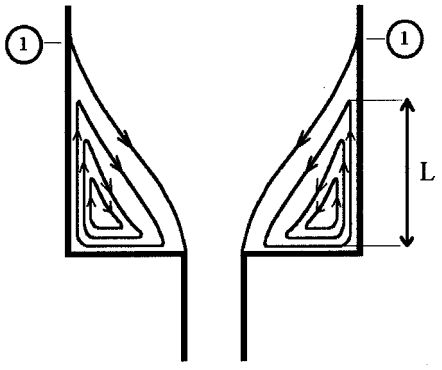

Fig. 15. Vortex size in a capillary.

If one uses a 180° entrance angle for the capillary, the vortex area is filled with blend material which is almost at rest (moderate shear). If one uses capillaries with smaller entrance angles, this vortex area is filled with metal from the capillary, leaving no space for blend material to collect. In this research a 180° entrance angle was used. It has been observed before (Bulters et al. [35], Binding et al. [36]) that the size of the vortex L (see Fig. 15) is related to a detachment point ① (see Fig. 15). The length L, of such a vortex can be described in a relatively easy way as discussed by Bulters et al. [35]. Here we limit ourselves to the main equations.

Bulters et al. [35] show that there is a strong analogy between the pullout phenomenon during spinning process and the occurrence of vortices in capillary entrances. Fig. 16 explains the correspondence. For pullout, the material is elongated by spinning, while air vortices are present in the remaining area within the capillary (②). An analogous deformation occurs with the melt in the contraction. The material is elongated and melt vortices occur in the edges of the capillary (①). When describing both phenomena, the detachment points ① and ② are very important. Pullout means that during spinning a melt from a capillary with a certain speed, the melt is not only elongated, but already starts to be spun to a smaller diameter within the capillary. In other words, the melt leaves the wall within the capillary at the detachment point ②.

At the detachment point the normal stress $\sigma_{rr} = 0$, while:

$$\sigma_{zz} = \frac{F}{\pi R^2} \tag{1}$$

with σ_{zz} the stress and F the force in the draw direction and R the radius of the fiber.

This gives for the first normal stress difference (N_1):

$$N_1 = \frac{F}{\pi R^2}. \tag{2}$$

If one uses a more accurate approach using a momentum

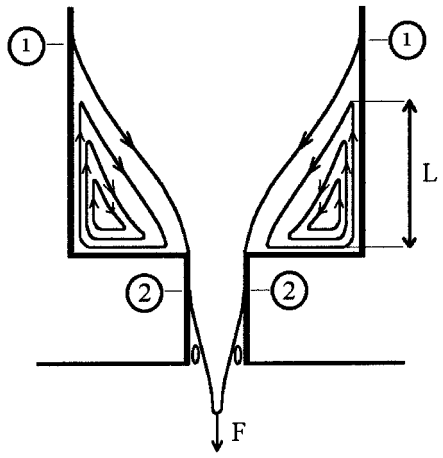

Fig. 16. Relation between pull out and vortex size (detachment points).

balance, one obtains:

$$F_c = 2\pi \int_0^R \left(N_1 + \frac{N_1}{2}\right) r \, dr \tag{3}$$

with the second normal stress difference $N_2 \approx -0.1N_1$, and F_c the critical force for leaving the wall. For a power law material, which is more or less the case for our blend system (see Fig. 4), the spinning force F can be calculated from:

$$v_0 = \frac{Q}{\pi R_0^2}, \tag{4}$$

$$\frac{v_1}{v_0} = \left(\frac{R_0}{R_1}\right)^2 \tag{5}$$

with v_1 the velocity in the capillary and v_0 the velocity in the reservoir, R_1 the capillary radius and R_0 the reservoir radius. Q is the throughput through the capillary.

$$\eta_e = \eta_{e0}\left(\frac{dv_z}{dz}\right)^{k-1} \tag{6}$$

η_e is the elongational viscosity and η_{e0} the prefactor for zero deformation rate, k is an index.

$$Q = A_0 v_0 = A_z v_z \tag{7}$$

where A_0 is the cross-section of the reservoir and A_z the cross-section of the capillary, v_z is the velocity in the capillary.

$$\sigma_{zz} = \frac{F}{A_z}. \tag{8}$$

This yields:

$$F = \frac{Q\eta_{e0}}{L} L^{\alpha}\left[\frac{1}{\alpha}\left(v_1^{\alpha} - v_0^{\alpha}\right)\right]^{1/(1-\alpha)} \qquad \alpha = \frac{k-1}{k}(\text{an index}) \tag{9}$$

Using the power law relations:

$$N_1 = \psi_0 \dot{\gamma}^m, \tag{10}$$

$$\eta = \eta_0 \dot{\gamma}^{n-1} \tag{11}$$

(m and n are power law indices, η_0 is the zero shear viscosity and ψ_0 is the zero shear normal stress) with Eqs. (3) and (6), this results in:

$$L = R_0 \frac{1}{4\alpha}\left[\left(\frac{R_0}{R_1}\right)^{2\alpha} - 1\right] \times \left[\eta_{e0}\frac{m+2n}{2\psi_0 n}\left(\frac{4n}{3n+1}\right)^m\right]^{1-\alpha}\left(\frac{4Q}{\pi R_0^3}\right)^{1-m(1-\alpha)}. \tag{12}$$

From this equation one can see a direct relation between L and p.s. applied, as Q is the only parameter that changes with changing piston speed (p.s.). This means that L increases with piston speed applied. This is in agreement with experimental results from Bulters et al. [35] and others. However, if piston speed is increased further, L becomes so large that a fluid instability can be observed within the capillary. This instability is illustrated in Fig. 17.

One can observe the melt whirling just above the capillary entrance region. With this whirl, the vortices with blend material almost at rest are rotated into the capillary. Most probably the samples of type *b* are mixed transparent material caused by the elongation in the die entrance, but with demixed bluish material wrapped around this coming from the vortices. The material is demixed at rest at these temperatures, so the vortex melt has comparable phase behaviour (demixed), responsible for the bluish curl observed.

Another indication for the occurrence of this melt instability is the shape of the samples coming out of the

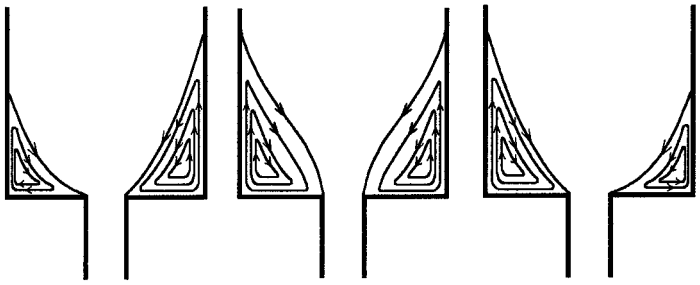

Fig. 17. Instability in contraction region, resulting in asymmetry in vortex size [37].

capillary. Samples of type *a* and d are straight smooth cylinders, while the type *b* samples are curled (Fig. 6).

The samples of type *c* are also curled, probably indicating that the same phenomenon occurs, but both the elongated and the vortex material are demixed. For this reason no discrepancy between the two types of material can be made by visual observation.

A temperature change will have its influence on η_{e0} and ψ_0, all other parameters in Eq. (12) remaining unchanged. It is known that the first normal stress difference is more sensitive to changes in temperature than viscosity. This means that an increase in temperature will decrease the ratio η_{e0}/ψ_0 and as a result will decrease L. In other words, at a higher temperature a higher piston speed is required to reach the same vortex size L where the whirl starts. This explains the shift of the type *b* boundary in Figs. 7–9 when going from 210°C to 220°C. It is not clear whether the area marked type *b* in Figs. 7–9 at $T = 230$°C is really of type *b* or whether it is an extension of the type *d* area with an opaque whirl around it because of the whirl in the capillary (i.e. not a transparent sample with an opaque whirl, but a deformation induced demixed blend with differently demixed material around it owing to the whirl). However there are two difficult points in this explanation. At $T = 190$°C and $T = 200$°C, type *b* behaviour was still found, while the stationary phase diagram shows that the blend should be mixed at these temperatures. This means that the material in the vortices should not be demixed. An explanation for this effect is not easy to find, but the material in the vortex is not really in rest. Perhaps low shear rates may cause the sample to demix in the vortices. However, at these temperatures only a few experiments up to modest piston speeds were performed because of pressure limitations (1800 bar). This brings us to a second difference with the PS/PVME experiments: the pressure influence on phase behaviour. In the experimental set-up used, pressure is present, while it is absent in the PS/PVME experiments of Fernandez et al. [1,24]. Pressure also could be a factor of influence here. Moreover some friction during the whirl movement could have caused local viscous heating causing the blend to phase separate. The latter explanation seems to be most plausible.

Secondly, for all temperatures, at the highest piston speeds used a homogeneously mixed material was always obtained. As pressure induces miscibility as far as we know [29–31], this could be an explanation for the absence of opaque curls in these samples.

The third difference between the theoretical and experimental results obtained for the PS/PVME system [1] and the ones discussed for the SMA/PMMA system is the difference in type of deformation applied. The PS/PVME experiments were pure shear experiments to maximum 10 s^{-1}. In this research apparent shear rates ranging from 0.6 to 25 000 s^{-1} were applied. Or, to be more precise, low to high deformation rates (piston speeds) were applied causing low to high elongational rates in the contraction and low to high shear rates in the capillary. The incorporation of elongation in the deformation process is especially interesting, as it corresponds to what happens in the nozzle of an injection moulding machine. This means that the complex diagrams, as shown before, are the result of predominantly elongational flow in the contraction followed by a shear in the capillary. For this reason it is difficult to discriminate between the influence of elongation and the influence of pure shear on the blend phase behaviour. However, the injection moulding experiments (Fig. 5, [32,33]) indicate that elongation has even more influence on blend phase behaviour than has shear, because it is found that the higher the contraction in the nozzle the more the sample phase separates.

Continuation of capillary experiments should focus on three different parameters. First the capillary length can be varied. If the capillary is very short, most of the deformation applied is elongation because of the contraction. In contrast, if a very long capillary is used, the influence of the elongation in the contraction can relax during flow in the long capillary and phase behaviour will be determined by shear. Secondly, by changing the capillary diameter the amount of contraction and thus elongation can be changed. Third, the entrance angle can be changed. This will show whether the theory of the whirl for type *b* samples is correct, because there will be no vortices for a small entrance angle.

5. Conclusions

Processing of a SMA/PMMA blend through a capillary results in a complex change of phase behaviour with deformation rate. Both deformation induced demixing and remixing are observed. This complex phase diagram as a function of apparent shear rate is in qualitative agreement with experimental and theoretical results found for a PS/PVME blend [1]. The only difference is the tongue shaped area in the complex phase diagram indicated as type *b* samples. This sample appearance can be related to the occurrence of vortices near the entrance of the capillary and is a phenomenon which will only occur in contraction flow experiments. Pure shear experiments, such as parallel plate or cone and plate, will not show such behaviour.

The deformation induced phase separation is spinodal phase separation. This can be concluded from light microscopy experiments and via reheating experiments, showing that the blend needed only 15–25 s to remix.

Indications were found that besides shear, elongation also causes dramatic changes in the blend phase behaviour. Capillary experiments are difficult to interpret because of the combination of shear, elongation, pressure and viscous heating. However, industrial scale processing such as injection moulding does show the same complexity in deformation, and hence capillary experiments are the best comparable experiment. Future experiments will focus on changing the capillary geometry in order to discriminate between the influence of shear and elongation.

Acknowledgements

The authors would like to thank J. Boyens for his continuing support and interest for this research, M. Bulters for his enormous help in understanding the samples with the bluish curl and theory on vortex size [35] and DSM Research for financial support.

References

[1] Fernandez ML, Higgins JS, Horst R, Wolf BA. Polymer 1995;36(1).
[2] Wolf BA, Kramer H. J Polym Sci Polym Lett 1980;18:789.
[3] Wolf BA. Macromolecules 1984;17:615.
[4] Kammer HW, Kummerloewe C, Kressler J, Melior JP. Polymer 1991;32(8):1488–1492.
[5] Horst R, Wolf BA. Macromolecules 1991;24:2236–2239.
[6] Horst R, Wolf BA. Macromolecules 1992;25:5291–5296.
[7] Evans DJ, Hanley HJM, Hess S. Phys Today 1984;37:26.
[8] Romig Jr KD, Hanley HJM. Int J Thermophys 1986;7:877.
[9] ver Strate G, Phillipoff WJ. J Polym Sci Polym Lett 1974;12:267.
[10] Silberberg A, Kuhn W. Nature 1952;170:450.
[11] Mani S, Malone MF, Winter HH, Halary JL, Monnerie L. Macromolecules 1991;24:5451.
[12] Hindawi I, Higgins JS, Galambos AF, Weiss RA. Macromolecules 1990;23:670–674.
[13] Mazich KA, Carr SH. J Appl Phys 1983;54:5511.
[14] Nakatani AI, Kim H, Takahashi Y, Matsushita Y, Takano A, Bauer BJ, Han CCJ. J Chem Phys 1990;93(1):795–810.
[15] Lyngaae-Jorgensen J, Sondergaard K. Polym Eng Sci 1987;27:344.
[16] Lyngaae-Jorgensen J, Sondergaard K. Polym Eng Sci 1987;27:351.
[17] Rangel-Nafaile C, Metzner AB, Wissbrun KF. Macromolecules 1984;17:1187.
[18] Krämer-Lucas H, Schenck H, Wolf BA. Makromol Chem 1988;189:1627–1634.
[19] Kramer H, Wolf BA. Makromol. Chem Rapid Commun 1985;6:21.
[20] Vrahopoulou-Gilbert E, McHugh AJ. Macromolecules 1984;17:2567.
[21] Mani S, Malone MF, Winter HH. Macromolecules 1992;25:5671–5676.
[22] Katsaros JD, Malone FM, Winter HH. Polym Eng Sci 1989;29(20):1434–1445.
[23] Hindawi IA, Higgins JS, Weiss RA. Polymer 1992;33(12):2522–2529.
[24] Fernandez ML, Higgins JS, Richardson SM. Trans IChemE 1993;71 Part A:239–244.
[25] Onuki A. Phys Rev Lett 1989;62(21):2472–2475.
[26] Hashimoto T, Takebe T, Fujioka K. In: Onuki A, Kawasaki K, editors. Springer proceedings in physics, Vol. 52, 1990.
[27] ten Brinke G, Szleifer I. Macromolecules 1995;28:5434–5439.
[28] Doi M, Onuki A. J Phys II France 1992;2:1631–1656.
[29] Schwahn D, Frielinghaus H, Mortensen K, Almdal K. Phys Rev Lett 1996;77(15):3153–3156.
[30] Frielinghaus H, Schwahn D, Mortensen K, Almdal K, Springer T. Macromolecules 1996;29:3263–3271.
[31] Janssen S, Schwahn D, Mortensen K, Springer T. Macromolecules 1993;26:5587–5591.
[32] Aelmans NJJ, Reid VMC. Abstract from poster presentation in conference book of the European Symposium on Polymer Blends, May 12–15 1996, Maastricht, The Netherlands.
[33] Aelmans NJJ, Reid VMC, Higgins JS. To be published.
[34] Horst R. Unpublished results, 1995.
[35] Bulters MJH, Meijer HEH. J of Non-Newtonian Fluid Mech 1990;38:43–80.
[36] Binding DM, Walters K. J of Non-Newtonian Fluid Mech 1988;30:233.
[37] Bulters MJH et al. Unpublished results.